



HAL
open science

Gold-Catalyzed 1,2-Aryl Shift and Double Alkyne Benzannulation

Gana Sanil, Maciej Krzeszewski, Wojciech Chaladaj, Witold Danikiewicz, Iryna Knysh, Łukasz Dobrzycki, Olga Staszewska-krajewska, Michal K Cyrański, Denis D Jacquemin, Daniel T Gryko

► **To cite this version:**

Gana Sanil, Maciej Krzeszewski, Wojciech Chaladaj, Witold Danikiewicz, Iryna Knysh, et al.. Gold-Catalyzed 1,2-Aryl Shift and Double Alkyne Benzannulation. *Angewandte Chemie International Edition*, 2023, 62 (49), 10.1002/anie.202311123 . hal-04845253

HAL Id: hal-04845253

<https://hal.science/hal-04845253v1>

Submitted on 18 Dec 2024

HAL is a multi-disciplinary open access archive for the deposit and dissemination of scientific research documents, whether they are published or not. The documents may come from teaching and research institutions in France or abroad, or from public or private research centers.

L'archive ouverte pluridisciplinaire **HAL**, est destinée au dépôt et à la diffusion de documents scientifiques de niveau recherche, publiés ou non, émanant des établissements d'enseignement et de recherche français ou étrangers, des laboratoires publics ou privés.



Distributed under a Creative Commons Attribution - NonCommercial 4.0 International License

Gold-Catalyzed 1,2-Aryl Shift and Double Alkyne Benzannulation

Gana Sanil, Maciej Krzeszewski,* Wojciech Chaładaj, Witold Danikiewicz, Iryna Knysh, Łukasz Dobrzycki, Olga Staszewska-Krajewska, Michał K. Cyrański, Denis Jacquemin,* and Daniel T. Gryko*

Dedicated to prof. Harry B. Gray on occasion of his 88th birthday

Abstract: The tandem intramolecular hydroarylation of alkynes accompanied by a 1,2-aryl shift is described. Harnessing the unique electron-rich character of 1,4-dihydropyrrolo[3,2-*b*]pyrrole scaffold, we demonstrate that the hydroarylation of alkynes proceeds at the already occupied positions 2 and 5 leading to a 1,2-aryl shift. Remarkably, the reaction proceeds only in the presence of cationic gold catalyst, and it leads to heretofore unknown π -expanded, centrosymmetric pyrrolo[3,2-*b*]pyrroles. The utility is verified in the preparation of 13 products that bear six conjugated rings. The observed compatibility with various functional groups allows for increased tunability with regard to the photophysical properties as well as providing sites for further functionalization. Computational studies of the reaction mechanism revealed that the formation of the six-membered rings accompanied with a 1,2-aryl shift is both kinetically and thermodynamically favourable over plausible formation of products containing 7-membered rings. Steady-state UV/Visible spectroscopy reveals that upon photoexcitation, the prepared S-shaped N-doped nanographenes undergo mostly radiative relaxation leading to large fluorescence quantum yields. Their optical properties are rationalized through time-dependent density functional theory calculations. We anticipate that this chemistry will empower the creation of new materials with various functionalities.

Introduction

The venerable polycyclic aromatic hydrocarbons (PAHs) and their heterocyclic analogs have garnered exceptional attention from the scientific community during the last decade.^[1–12] Among dozens of key reactions which are employed to assemble these dyes, alkyne benzannulation (intramolecular hydroarylation of alkynes) discovered by Swager in 1994^[13,14] is one of the most universal approaches. Over the years a panel of different catalysts belonging to either Brønsted acids or Lewis acids were introduced. As a result, alkyne benzannulation has been used to form various nanographenes.^[15–20] Among several emblematic examples, a spectacular illustration concerns the synthesis of a polymeric graphene nanoribbon by Chalifoux and co-workers.^[21] This reaction has also been used to assemble S-doped^[22,23] and N-doped nanographenes,^[24] and, more recently, for the construction of helicenes.^[25–28] Alkyne benzannulation occurs at the free position adjacent to the biaryl linkage leading to the formation of new rings of various sizes. Depending on the conditions and the catalyst used in the reaction, 5-, 6- and 7-membered rings can be formed through 5-*exo-dig*, 6-*endo-dig* and 7-*endo-dig* ring closure mechanisms, respectively (Figure 1a).^[17,19,23,25,28,29]

Double 6-*endo-dig* cyclizations are also known, including impressive domino twofold cyclization reported by Chalifoux (Figure 1b),^[19] or our previous work where two six-membered rings were fused to the central pyrrolopyrrole core (Figure 1c).^[30] Tetraarylpyrrolo[3,2-*b*]pyrroles (TAPPs)^[31,32] are being applied as scaffolds to prepare numerous N-doped nanographenes, owing to the intrinsic reactivity of positions 3 and 6, the ability to introduce sterically hindered substituents and its high amenability to

[*] G. Sanil, Dr. M. Krzeszewski, Dr. W. Chaładaj, Prof. W. Danikiewicz, Dr. O. Staszewska-Krajewska, Prof. D. T. Gryko
Institute of Organic Chemistry, Polish Academy of Sciences
Kasprzaka 44/52, 01-224 Warsaw (Poland)
E-mail: mkc@chem.uw.edu.pl
dtrgyko@icho.edu.pl

I. Knysh, Prof. D. Jacquemin
Nantes Université, CNRS, CEISAM UMR 6230,
F-44000 Nantes (France)
E-mail: denis.jacquemin@univ-nantes.fr

Dr. Ł. Dobrzycki, Prof. M. K. Cyrański
Faculty of Chemistry, University of Warsaw,
Pasteura 1, 02-093 Warsaw (Poland)

Prof. D. Jacquemin
Institut Universitaire de France (IUF), F-75005 Paris (France)
E-mail: denis.jacquemin@univ-nantes.fr

© 2023 The Authors. Angewandte Chemie International Edition published by Wiley-VCH GmbH. This is an open access article under the terms of the Creative Commons Attribution Non-Commercial License, which permits use, distribution and reproduction in any medium, provided the original work is properly cited and is not used for commercial purposes.

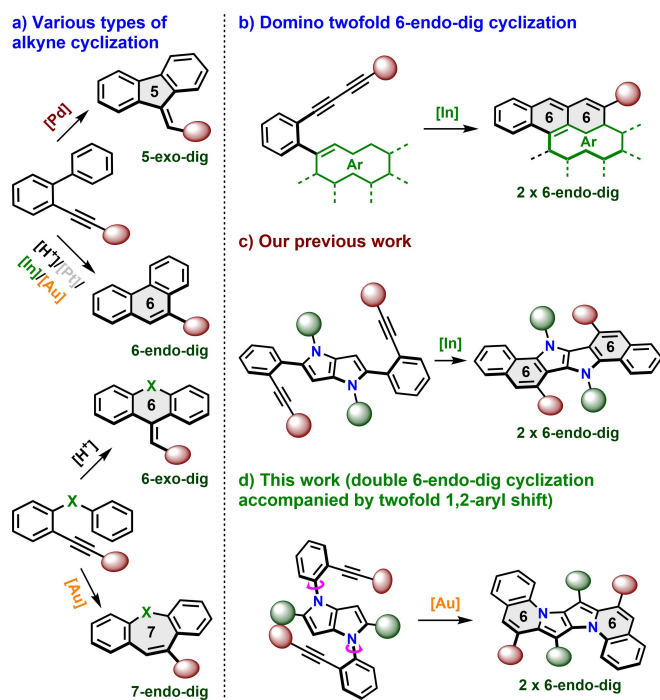


Figure 1. Intramolecular cyclization of alkynes under various conditions leading to the formation of one new 5-, 6- or 7-membered rings or two 6-membered rings at once.

chemical modifications.^[33–35] Taking advantage of this new chemical space, enabled by a multicomponent reaction leading to 1,4-dihydropyrrolo[3,2-*b*]pyrroles (DHPPs)^[36,37] we hypothesized that it could be possible to obtain π -expanded DHPPs possessing fused five- and seven-membered rings.^[38–40] Assessing this hypothesis requires DHPPs possessing aryethynylaryl substituents at positions 1 and 4 which could undergo double alkyne benzannulation forming two 7-membered rings (Figure 1d, Figure 2).

It turned out, however, that the obtained compounds comprised of two six-membered rings fused to the central core. Herein we present the double intramolecular cyclization of alkynes via cyclization at the already occupied positions C2/C5 with a consequent double aryl shift from position C2/C5 to C3/C6.

Results and Discussion

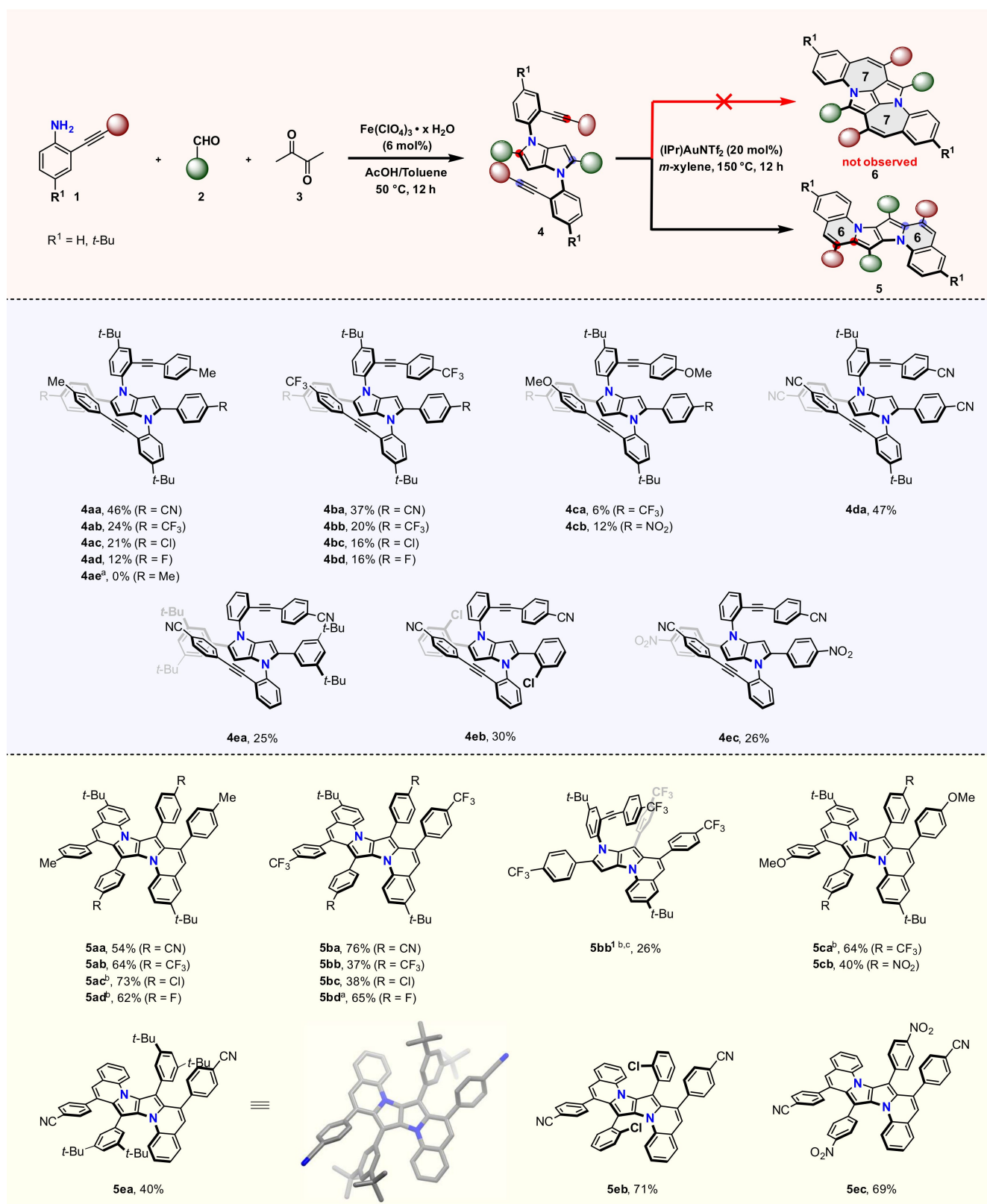
Design and Synthesis

A two-step strategy comprising of a multicomponent reaction affording TAPPs followed by double alkyne benzannulation was thought to present an ideal synthetic platform for modular access to the envisioned dyes (Figure 2). Our synthetic approach capitalizes on the inherently electron-rich positions 3 and 6 of DHPPs and the direct access to TAPPs possessing diphenylethyne moieties at positions 1 and 4 (Figure 2). This enables to position the carbon-carbon triple bond in proximity to the free positions 3 and 6, thus

facilitating the formation of seven-membered rings during the hydroarylation. The designed protocol initiates with the synthesis of 2-(phenylethynyl)anilines **1a–e**. Amines **1a–d** were synthesized via Sonogashira reaction using the corresponding 4-*tert* butyl-2-iodoaniline and rationally chosen ethynylbenzenes possessing both electron-donating and electron-withdrawing substituents in the *para*-position. For the synthesis of amine **1e**, however we resort to the sila-Sonogashira variant, namely, 2-((trimethylsilyl)ethynyl)aniline and 4-bromobenzonitrile as a coupling partner. In light of our previous experiences, the introduction of alkyl groups such as *tert*-butyl has a significant impact on increasing the solubility of extended aromatic systems by preventing π -stacking.^[30] With the amines **1a–e** in hand, by employing our multicomponent reaction^[41] we readily prepared a library of tetraarylpyrrolo[3,2-*b*]pyrroles (TAPPs) **4aa–4ec** in yields ranging from 6 to 47%. In most of the cases, the products were precipitated in the reaction mixture and further purified by recrystallization (see the ESI for details).

In order to perform the envisioned double intramolecular hydroarylation, we initially relied on the use of π -Lewis acids such as PtCl_2 ,^[42,43] InCl_3 , and GaCl_3 , primarily used for 6-*endo* annulation reported by Fürstner and co-workers.^[42,44] The choice of catalysts was based on the literature and our previous reports of successful hydroarylation strategies on structurally similar TAPPs.^[30] Unfortunately, none of the attempts led to any conversion. Subsequent studies involving Brønsted acids (i.e. trifluoroacetic acid and *p*-toluenesulfonic acid) and neutral chlorogold(I) catalysts (e.g., $\text{AuCl}(\text{PPh}_3)$)^[45–48] were also unsuccessful. Even increasing the temperature to 150 °C did not result in any conversion of TAPP **4aa** (see the ESI). Steric hindrance around the reaction center may account for the failure of this reaction. Murakami and co-workers reported hydroarylation of dialkynylbiphenyls for the synthesis of aryl substituted pyrenes using cationic (SPhos)AuNTf₂ catalyst.^[49] By employing the same conditions with electronically analogous IPrAuNTf_2 as the catalyst, the transformation of substrate **4ea** into a new substance was observed. The primary analysis of ¹H NMR (showing small number of peaks denoting the symmetry and the absence of pyrrolic singlet around 6.0–6.5 ppm) and matching HRMS-EI (Calculated for $\text{C}_{64}\text{H}_{60}\text{N}_4^{+}$: $[\text{M}]^{+} = 884.4812$, found = 884.4840) of the obtained compound apparently supported our assumption of the formation of seven membered ring. Surprisingly, X-ray crystallography analysis disproved our prediction (Figure 2).^[50] It became clear that two new six-membered rings were formed at the central core of the compound **4ea** leading to an S-shaped non-planar π -expanded DHPP. 6-*Endo* cyclization occurs at the already occupied C2/C5 positions simultaneously inducing the double aryl shift from positions C2/C5 to C3/C6.

It is pivotal to emphasize that already in 1997 Swager and co-workers reported rearrangements during alkyne hydroarylations.^[13] Recently Chalifoux and co-workers revealed the 1,2-shift occurring during four-fold alkyne benzannulation leading to pyreno[*a*]pyrene-based helicene hybrids.^[51] Processes reported by Swager and Chalifoux are most probably the proton-mediated reactions rather than an



in situ rearrangement. An analogous 1,2-migration of alkyl or aryl groups was observed in the gold-catalyzed intramolecular cascade cyclization assisted by heteronucleophiles.^[29,52] In broader context, one has to point out that 1,2-aryl shift of halides were reported multiple times by the groups of Fürstner, Müllen, Davis etc.^[42,53–55] The recent revival of interest in gold catalysis led to important findings which reveal that gold(I) complexes are prone to induce various rearrangements^[56] and that the interplay between gold catalysis and protic acids catalysis is rather complex.^[57,58]

To further demonstrate functional group compatibility and synthetic utilization, after establishing the protocol, the reaction was performed on the previously synthesized TAPPs bearing various substituents at the periphery. The reaction turned out to be general in most of the cases and the rearranged products **5aa–ec** were formed in reasonable yields ranging from 27–76% (Figure 2). The only case where the reaction did not proceed to completion was that of TAPP **4da** bearing four cyano groups at the periphery. The presence of highly electron withdrawing groups in the *para*-position to the carbon atom attached to the alkyne and on the migrating aryl substituents might affect the nucleophilicity of the system by preventing the reaction from proceeding towards completion. The reaction mixture showed the presence of parent TAPP even after 48 hours of reaction time. The extremely low solubility of both the product and reactant in common organic solvents made the purification process impossible. Interestingly, for the compound **4bb**, we could obtain the mono-fused unsymmetrical DHPP **5bb'** by lowering the reaction time to 4 hours. This shows the tunability of the reaction by time and confirms that the aryl-shift occurs in a stepwise manner. It is worth mentioning that the formation of the product **5eb** bearing *ortho*-chlorine substituents in high yield (71%) depicts the efficiency of this reaction even with the steric hindrance close to the migration center. This also broadens its synthetic potential for further transformations. If two arylolethynyl groups differing in an electronic effect (i.e. 4-CF₃C₆H₄ and 4-MeOC₆H₄) are present in the starting TAPP, double benzannulation occurs smoothly leading to expected rearranged product, with no apparent regio- and chemoselectivity. Shortening the reaction time to 2 h did not enable to isolate any intermediate products (see the ESI for details).

No other identifiable products have been detected in any of these reactions. In our opinion the key reason responsible for the low yields of the products is that double alkyne benzannulation accompanied by 1,2-aryl shift is very demanding. Indeed it does not occur with any other Brønsted or Lewis acid employed (ESI, Table S1), even at very high temperature. The only exception is the prolonged heating of TAPP **4aa** with HNTf₂ at 150°C which led to approx. 10% of conversion. Control experiments when both IPrAuNTf₂ and several Brønsted or Lewis acid were simultaneously employed led to the same results as with gold-based catalyst only (Table S2). On the other hand the addition of NaHCO₃ has no effect and the addition of

organic base has marginal effect on the reaction conversion (Table S3).

Computational Studies—Mechanism

To rationalize observed *6-endo-dig* benzannulation merged with aryl shift, ultimately providing **5**, rather than expected *7-endo-dig* cyclization leading to **6**, both mechanistic scenarios were investigated computationally (Figure 3, black and grey paths, respectively). The calculations were performed on model substrate **7**, bearing no substituents on benzene rings, and full structure of gold catalyst (IPrAuNTf₂).

Both paths start from endoergic displacement of triflimide anion by alkyne moiety of **7** giving rise to the corresponding π -complex **8** or **8a**. Coordination of cationic gold motif to C–C triple bond triggers intramolecular nucleophilic attack of electron-rich pyrrolopyrrole system on the activated alkyne moiety of **8** through a *6-endo-dig* manifold. The process leading to the formation of intermediate **9** proceed through a transition state **TS1** ($\Delta G^\ddagger = 159.6$ kJ/mol, from **7**). The subsequent 1,2-aryl shift delivers **10** via **TS2** with Gibbs free energy of activation of 74.3 kJ/mol. Finally, abstraction of proton from the position 3 of the pyrrolopyrrole scaffold followed by protodeauration liberates catalyst and compound **11**, product of single *6-endo-dig* benzannulation of **7**. Analogical sequence of reactions triggered by coordination of cationic gold complex to the alkyne motif in **11** delivers final product **12**. Noticeably, the overall transformation of **7** involving one or two sequences of hydroarylation of alkynes accompanied by a 1,2-aryl shift, leading to **11** and **12** is highly exergonic ($\Delta G = -165.2$ and -301.3 kJ/mol, respectively).

Alternatively, *7-endo-dig* cyclization of **8a** (conformer of **8**) towards intermediate **10a** proceeds through a transition state **TS3** ($\Delta G^\ddagger = 177.6$ kJ/mol, from **7**) lying 18 kJ/mol higher than **TS1** (leading to **10** via *6-exo-dig* process). Such a difference in the reaction barriers correspond to selectivity higher than 160:1 at 150°C. Moreover, due to strain and steric hindrance of intermediate **10a** bearing 7-membered ring is also considerably less thermodynamically stable than both **9** and **10**. The hypothetical product **11a** is liberated through a sequence of deprotonation followed by protodeauration, and can enter a second event of *7-endo-dig* benzannulation giving rise to **12a**. Noticeably, formation of **11a** and **12a** is not only kinetically unfavourable compared to **11** and **12**, but also thermodynamically less preferred ($\Delta G = -80.2$ and -166.2 kJ/mol for **11a** and **12a** vs -165.2 and -301.3 kJ/mol for **11** and **12**, respectively).

Photophysical Properties

For TAPPs possessing electron-withdrawing substituents at positions 2 and 5 and electron-neutral arylolethynylaryl substituents at positions 1 and 4 the absorption and emission characteristics are different than for analogs bearing simple phenyl substituents at positions 1 and 4. The direct comparison of TAPP **4aa** ($\lambda_{\text{abs}}^{\text{max}} = 410$ nm and $\lambda_{\text{em}}^{\text{max}} = 450$ nm in

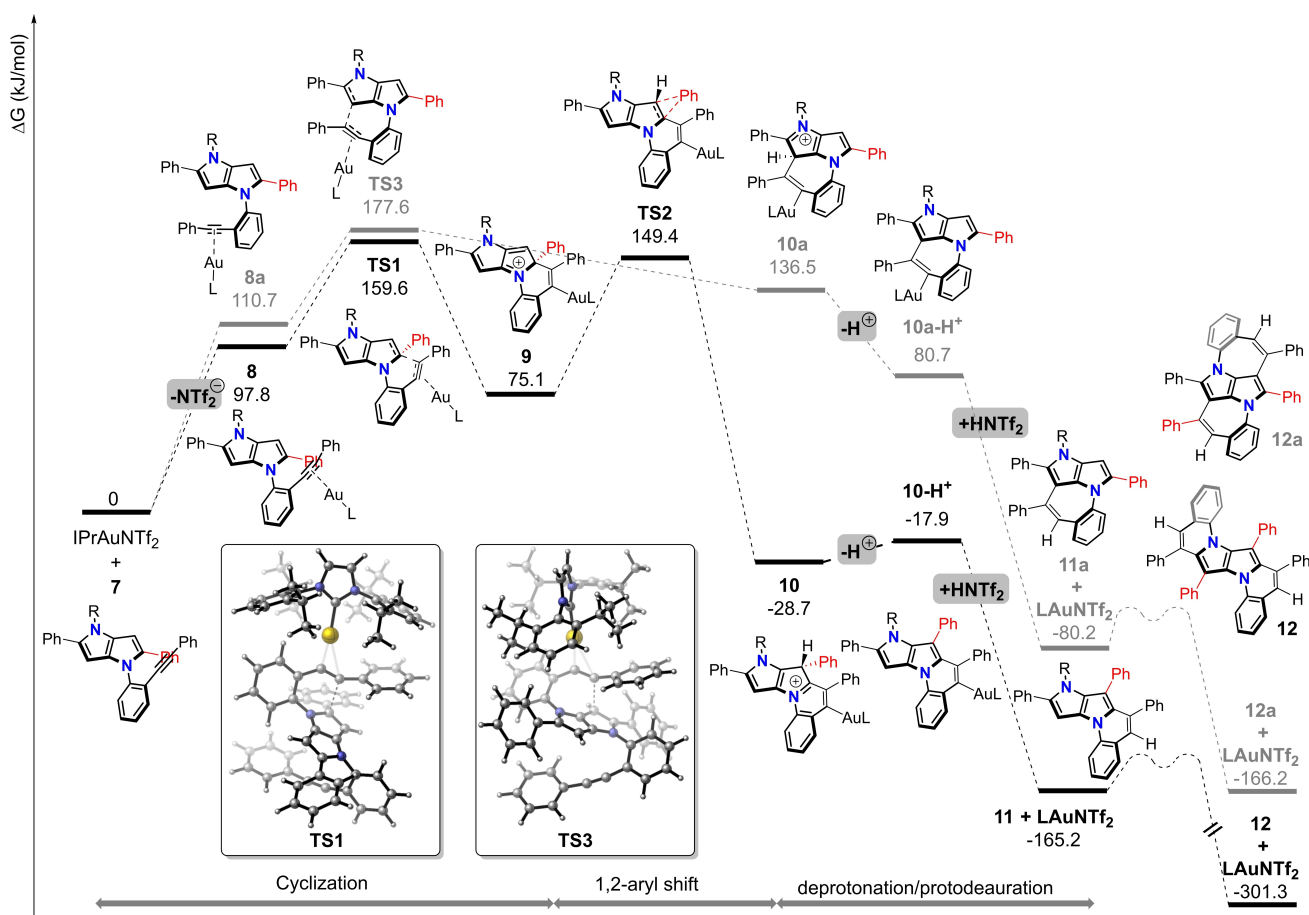


Figure 3. Gibbs free energy profiles for two plausible 6-endo-dig and 7-endo-dig benzannulations of **7** catalyzed by the IPrAuNTf₂. Calculated at SMD(m-xylene)/M06/def2-TZVPP//B3LYP-D3/def2-SVP level of theory.

toluene) with model 1,4-di(4-methylphenyl)-2,5-di(4-cyanophenyl)-1,4-dihydropyrrolo[3,2-*b*]pyrrole^[59] reveals that both absorption and emission are bathochromically shifted, by 20 nm and 50 nm respectively (Table S5, Figure 4). In analogy with parent TAPP, both emission maximum and fluorescence quantum yield (ϕ_f) for TAPP **4aa** are insensi-

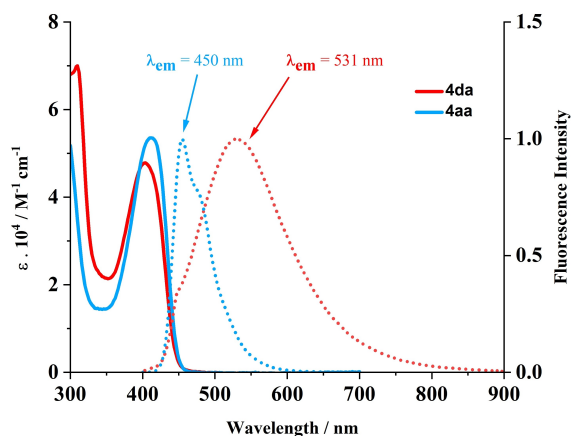


Figure 4. UV/Vis absorption spectra (solid lines) and fluorescence spectra (dotted lines) of compounds **4da** and **4aa** measured in THF.

tive to solvent polarity change.^[60] An analogous observation can be performed for **4ab**. Strikingly a different situation occurs when 4-cyanophenyl substituents are present at position 1 and 4. In the case of TAPP **4da** whereas $\lambda_{\text{abs}}^{\text{max}}$ is located at the same position (408 nm), $\lambda_{\text{em}}^{\text{max}}$ is already bathochromically shifted in toluene to 472 nm and this effect becomes pronounced in THF (531 nm, see Table S5 and Figure 4). At the same time ϕ_f decreases in polar THF >10-fold unlike in the case of **4aa**. Close examination of the remaining TAPPs (e.g. **4bb**, **4bc**, **4bd**, etc.) shows that the presence of electron-withdrawing substituents (4-CNC₆H₄ and 4-CF₃C₆H₄) at positions 1 and 4 always induces large bathochromic shift of fluorescence in polar solvents (THF). Since through-bond electronic communication cannot be too strong due to the large dihedral angle, this indicates a through-space interaction, as confirmed by theoretical calculations (see below). Intriguingly, in some of these cases, ϕ_f is very small which again does not resemble many parent analogs.^[59] Yet different observations are noted in the case of TAPPs **4cb** and **4ec** bearing 4-nitrophenyl substituents at position 2 and 5. Regardless of the electronic character of substituents present at positions 1 and 4 the fluorescence is essentially quantitative in toluene and very weak in THF.^[61]

Needless to say, the fused dyes **5** possess a more rigid structure and they can be considered analogs of π -expanded

DHPPs synthesized in 2015.^[62] For these fused architectures, the low energy absorption band is located at ca. 480 nm and it has a pronounced vibronic structure and very small Stokes shifts (Table S5, Figure 5). Dyes **5** are generally characterized by strong green emission with ϕ_{fl} typically above 0.75. The substituents at positions 3 and 6 do not strongly influence the photophysical properties (**5aa** vs. **5ad**). The presence of 4-nitrophenyl substituent at these positions (**5cb** vs. **5ec**) leads to the quenching of emission (ϕ_{fl} below the detection limit), whereas 4-cyanophenyl substituent at positions 3 and 6 (**5ba**, **5aa**) have negligible effect on the photophysics. Compared with X-shaped π -expanded pyrrolopyrroles,^[62] dyes **5** are ≈ 100 nm bathochromically shifted for both absorption and emission.

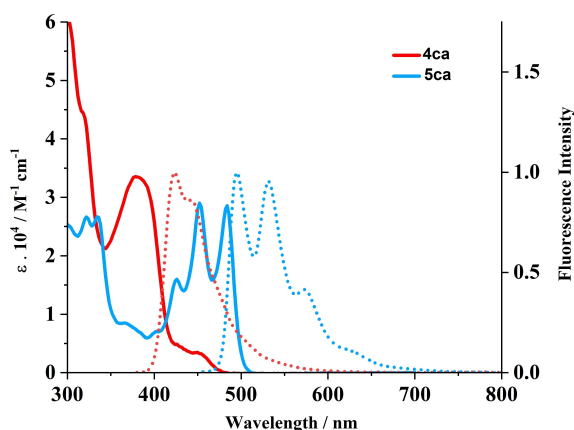


Figure 5. UV/Vis absorption spectra (solid lines) and fluorescence spectra (dotted lines) of compounds **4ca** and **5ca** measured in toluene.

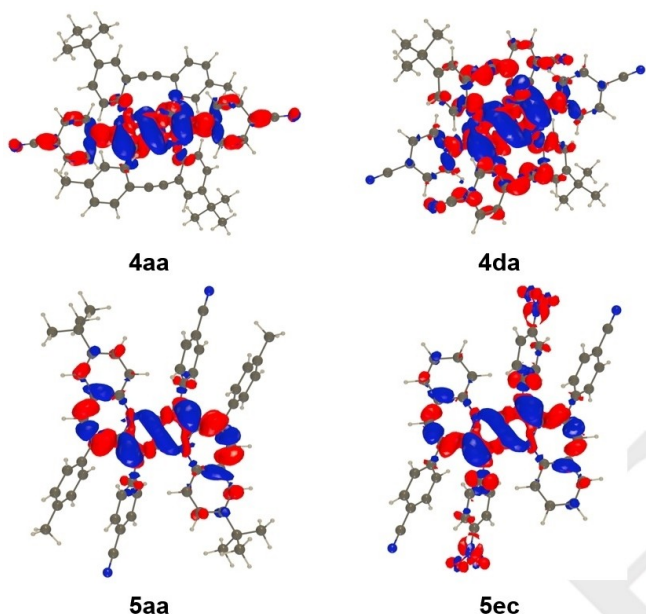


Figure 6. EDD plots for selected compounds. Navy blue and crimson red are regions of decrease and increase of density upon excitation. See the ESI for additional examples.

Computational Studies—Photophysics

We have used time-dependent density functional theory (TD-DFT)^[63] and second-order coupled-cluster (CC2)^[64] to model the photophysical properties of the selected compounds, accounting for solvent effects are the cLR²-PCM level^[65] (see the ESI). Figure 6 provides electron density difference (EDD) plots for **4aa** and **4da**. Both compounds show a large twist (56°) between the benzene rings at position 1 and 4, and the DHPP core preventing strong conjugation, yet their EDDs differ. In **4aa**, the excited state is delocalized on the central unit, the DHPP acting as the donor group and the benzonitrile moieties acting as acceptors, leading to the expected quadrupolar CT. This is consistent with the experimental findings that **4aa** essentially behaves like a standard quadrupolar centrosymmetric TAPP. In contrast in **4da**, one clearly notices a change of topology, the CT occurring *through-space*, from the DHPP moiety towards the 4-CNC₆H₄ groups attached through position 1 and 4, rather than the groups at position 2 and 5. According to Le Bahers' metric, the amount of charge transferred also increases from 0.67 e in **4aa** to 0.86 e in **4da**.

As expected, the hydroarylation leads to a strong decrease of the twist between the *N*-substituent and the core (ca. 15° instead of ca. 56°), with the excited states delocalized along the longer quasi-planar π -conjugated path (Figure 6). Interestingly, the EDDs show that the cyano group at positions 3 and 6 are not strong enough (as electron-withdrawing groups) to influence the topology of the electron distribution, whereas nitro groups do alter the photophysics of π -expanded DHPPs (**5aa** versus **5ec**). The significant contributions of the nitro groups in the excited state are consistent with the quenching of the emission in **5ec** (Table S5).

More quantitative comparisons between theory and experiments can be obtained by using 0–0 energies and band topologies. For the former, our calculations report values of ca. 2.5 eV for **4aa** and **4ba** but values around 2.2 eV for compounds of series **5** (**5aa**, **5ea**, **5eb**, and **5ec**, see Table S6 in the ESI). In particular, the **4aa** to **5aa** redshift is -0.38 eV, which perfectly fits the measurements of -0.36 eV. This redshift is a clear consequence of the planarization of the system. On the other hand, for **4da**, theory overshoots the experimental redshift of the emission due to the CT nature, but yields a fluorescence associated with a small oscillator strength, consistent with the decrease of emission yield noticed experimentally. Figure 7 shows the computed band shapes for the analogous **4aa** and **5aa**, and the more pronounced vibronic progression in the latter also appears clearly, as in Figure 5. In **5aa**, the vibronic shapes are mainly related to vibrations at ca. 1500–1600 cm⁻¹ involving changes in the alternation of single and double CC bonds (see the ESI), as expected for a π -conjugated dye. Interestingly for **5ea**, the fact that the absorption spectrum is more resolved than its fluorescence counterpart is well reproduced by the calculations (see the ESI), an outcome that we attribute to the loss of symmetry taking place in the excited state of **5ea** (and not in **5aa**).

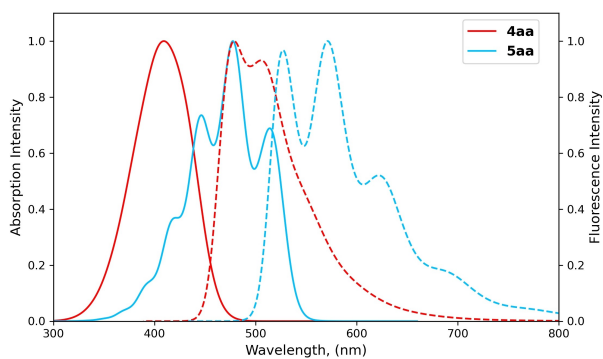


Figure 7. Vibrationally resolved spectra in toluene of **4aa** and **5aa** determined using the VG PES model on the basis of TD-DFT vibrations and CC2-corrected adiabatic energies.

Conclusion

The presence of a 1,4-dihydropyrrolo[3,2-*b*]pyrrole core alters the course of intramolecular hydroarylation of alkynes. Reactions leading to the anticipated formation of two seven-membered rings, instead, proceeds via a 1,2-aryl shift and six-membered rings are formed. Substituents present initially at positions 2 and 5 migrate to positions 3 and 6. In addition to uncovering the special example of a 1,2-aryl shift during the hydroarylation of alkynes, we identified that this reaction is tolerant to many functional groups, in particular those that are viable in the area of optoelectronics. This reaction leads to heretofore unknown heterocyclic skeletons, the structure of which consists of six conjugated aromatic rings. These results, combined with earlier examples of the Scholl reaction occurring with concomitant 1,2-aryl shift,^[66,67] suggests that the exceptional electron-rich character of DHPP core is responsible for this reaction course. Moreover, in all cases, the reaction led exclusively to the formation of 6-*endo-dig* cyclization products, and the possible 5-*exo* isomers were not detected. Importantly we successfully deciphered the mechanistic rationale behind the reaction, via computational studies. Critically, the properties of the benzannulation substrates i.e. sterically congested tetraaryl-1,4-dihydropyrrolo[3,2-*b*]pyrroles are controlled by both the strongly conjugated substituents at positions 2 and 5 and by weakly conjugated substituents at positions 1 and 4. We showed that the fluorescence of TAPPs possessing electron-withdrawing arylolethynyl substituents at positions 1 and 4 could plausibly be rationalized by a through-space interaction. Although certain substrate limitations exist, the findings will provide impetus for future explorations that use alkyne benzannulation. Collectively these results highlight the compatibility of exceptionally electron-rich heterocycles with Au(I)-catalyzed alkynyl hydroarylation.

Supporting Information

The authors have cited additional references within the Supporting Information.^[68–89]

Author Contributions

The manuscript was written through contributions of all authors. All authors have given approval to the final version of the manuscript.

Acknowledgements

This project has received funding from EU's Horizon 2020 research and innovation programme under Grant Agreement No 860762. The work was financially supported by the Polish National Science Centre, Poland (HARMONIA 2018/30/M/ST5/00460), the Foundation for Polish Science (TEAM POIR.04.04.00-00-3CF4/16-00 and START scholarship no. 039.2017 to M.K.). M.K. is a recipient of a scholarship awarded by the Polish Ministry of Education and Science to outstanding young scientists. I.K. and D.J. thank the French *Agence Nationale de la Recherche* (ANR) for support under contract No. ANR-20-CE29-0005 (BSE-Forces). This work used the computational resources of the CCIPL/GlicID mesocenter installed in Nantes. DFT calculations were carried out using resources provided by Wrocław Centre for Networking and Supercomputing (grant no. 518). The authors thank Joseph Milton for proofreading the manuscript.

Conflict of Interest

The authors declare no conflict of interest.

Data Availability Statement

The data that support the findings of this study are available in the supplementary material of this article.

Keywords: Alkynes · Biaryls · Dyes/Pigments · Fluorescence · Heterocycles

- [1] K. P. Kawahara, W. Matsuoka, H. Ito, K. Itami, *Angew. Chem. Int. Ed.* **2020**, *59*, 6383–6388.
- [2] K. Oki, M. Takase, S. Mori, H. Uno, *J. Am. Chem. Soc.* **2019**, *141*, 16255–16259.
- [3] A. Caruso, J. D. Tovar, *Org. Lett.* **2011**, *13*, 3106–3109.
- [4] A. Fukazawa, S. Yamaguchi, *Chem. Asian J.* **2009**, *4*, 1386–1400.
- [5] M. Navakouski, H. Zhylitskaya, P. J. Chmielewski, T. Lis, J. Cybińska, M. Stępień, *Angew. Chem. Int. Ed.* **2019**, *58*, 4929–4933.
- [6] S. Mishra, M. Krzeszewski, C. A. Pignedoli, P. Ruffieux, R. Fasel, D. T. Gryko, *Nat. Commun.* **2018**, *9*, 1714.
- [7] M. Stępień, E. Gońka, M. Żyła, N. Sprutta, *Chem. Rev.* **2017**, *117*, 3479–3716.
- [8] T. Hensel, N. N. Andersen, M. Plesner, M. Pittelkow, *Synlett* **2016**, *27*, 498–525.
- [9] E. Gońka, P. J. Chmielewski, T. Lis, M. Stępień, *J. Am. Chem. Soc.* **2014**, *136*, 16399–16410.

- [10] G. E. Rudebusch, A. G. Fix, H. A. Henthorn, C. L. Vonnegut, L. N. Zakharov, M. M. Haley, *Chem. Sci.* **2014**, *5*, 3627–3633.
- [11] G. Li, Y. Wu, J. Gao, J. Li, Y. Zhao, Q. Zhang, *Chem. Asian J.* **2013**, *8*, 1574–1578.
- [12] J. Fan, L. Zhang, A. L. Briseno, F. Wudl, *Org. Lett.* **2012**, *14*, 1024–1026.
- [13] M. B. Goldfinger, K. B. Crawford, T. M. Swager, *J. Am. Chem. Soc.* **1997**, *119*, 4578–4593.
- [14] M. B. Goldfinger, T. M. Swager, *J. Am. Chem. Soc.* **1994**, *116*, 7895–7896.
- [15] N. K. Saha, T. H. Barnes, L. J. Wilson, B. L. Merner, *Org. Lett.* **2022**, *24*, 1038–1042.
- [16] Y. Gu, V. Vega-Mayoral, S. Garcia-Orrit, D. Schollmeyer, A. Narita, J. Cabanillas-González, Z. Qiu, K. Müllen, *Angew. Chem. Int. Ed.* **2022**, *61*, e202201088.
- [17] K. M. Magiera, V. Aryal, W. A. Chalifoux, *Org. Biomol. Chem.* **2020**, *18*, 2372–2386.
- [18] J. Gicquiaud, A. Hacıhasanoğlu, P. Hermange, J. M. Sotiropoulos, P. Y. Toullec, *Adv. Synth. Catal.* **2019**, *361*, 2025–2030.
- [19] W. Yang, R. Bam, V. J. Catalano, W. A. Chalifoux, *Angew. Chem. Int. Ed.* **2018**, *57*, 14773–14777.
- [20] W. Yang, R. R. Kazemi, N. Karunathilake, V. J. Catalano, M. A. Alpuche-Aviles, W. A. Chalifoux, *Org. Chem. Front.* **2018**, *5*, 2288–2295.
- [21] W. Yang, A. Lucotti, M. Tommasini, W. A. Chalifoux, *J. Am. Chem. Soc.* **2016**, *138*, 9137–9144.
- [22] Y. Li, A. Concellón, C. J. Lin, N. A. Romero, S. Lin, T. M. Swager, *Chem. Sci.* **2020**, *11*, 4695–4701.
- [23] K. Sprenger, C. Golz, M. Alcarazo, *Eur. J. Org. Chem.* **2020**, 6245–6254.
- [24] J. Labella, G. Durán-Sampedro, S. Krishna, M. V. Martínez-Díaz, D. M. Guldi, T. Torres, *Angew. Chem. Int. Ed.* **2023**, *62*, e202214543.
- [25] E. González-Fernández, L. D. M. Nicholls, L. D. Schaaf, C. Farès, C. W. Lehmann, M. Alcarazo, *J. Am. Chem. Soc.* **2017**, *139*, 1428–1431.
- [26] M. Satoh, Y. Shibata, K. Tanaka, *Chem. Eur. J.* **2018**, *24*, 5434–5438.
- [27] T. Ikai, K. Oki, S. Yamakawa, E. Yashima, *Angew. Chem. Int. Ed.* **2023**, *62*, e202301836.
- [28] L. D. M. Nicholls, M. Marx, T. Hartung, E. González-Fernández, C. Golz, M. Alcarazo, *ACS Catal.* **2018**, *8*, 6079–6085.
- [29] A. S. Dudnik, V. Gevorgyan, *Angew. Chem. Int. Ed.* **2007**, *46*, 5195–5197.
- [30] R. Stézycki, M. Grzybowski, G. Clermont, M. Blanchard-Desce, D. T. Gryko, *Chem. Eur. J.* **2016**, *22*, 5198–5203.
- [31] G. Sanil, B. Koszarna, Y. M. Poronik, O. Vakuliuk, B. Szymański, D. Kusy, D. T. Gryko, *Adv. Heterocycl. Chem.* **2022**, *138*, 335–409.
- [32] S. Stecko, D. T. Gryko, *JACS Au* **2022**, *2*, 1290–1305.
- [33] M. Krzeszewski, Ł. Dobrzycki, A. L. Sobolewski, M. K. Cyrański, D. T. Gryko, *Angew. Chem. Int. Ed.* **2021**, *60*, 14998–15005.
- [34] M. Tasiór, M. Chotkowski, D. T. Gryko, *Org. Lett.* **2015**, *17*, 6106–6109.
- [35] M. Tasiór, P. Kowalczyk, M. Przybył, M. Czichy, P. Janasik, M. H. E. Bousquet, M. Łapkowski, M. Rammo, A. Rebane, D. Jacquemin, D. T. Gryko, *Chem. Sci.* **2021**, *12*, 15935–15946.
- [36] M. Krzeszewski, M. Tasiór, M. Grzybowski, D. T. Gryko, *Org. Synth.* **2021**, *98*, 242–262.
- [37] A. Janiga, E. Glodkowska-Mrowka, T. Stoklosa, D. T. Gryko, *Asian J. Org. Chem.* **2013**, *2*, 411–415.
- [38] H. Luo, J. Liu, *Angew. Chem. Int. Ed.* **2023**, *62*, e202302761.
- [39] C. Wang, Z. Deng, D. L. Phillips, J. Liu, *Angew. Chem. Int. Ed.* **2023**, *62*, e202306890.
- [40] Chaolumen, I. A. Stepek, K. E. Yamada, H. Ito, K. Itami, *Angew. Chem. Int. Ed.* **2021**, *60*, 23508–23532.
- [41] M. Tasiór, O. Vakuliuk, D. Koga, B. Koszarna, K. Górski, M. Grzybowski, Ł. Kielesiński, M. Krzeszewski, D. T. Gryko, *J. Org. Chem.* **2020**, *85*, 13529–13543.
- [42] V. Mamane, P. Hannen, A. Fürstner, *Chem. Eur. J.* **2004**, *10*, 4556–4575.
- [43] G. Wu, A. L. Rheingold, S. J. Geib, R. F. Heck, *Organometallics* **1987**, *6*, 1941–1946.
- [44] A. Fürstner, V. Mamane, *J. Org. Chem.* **2002**, *67*, 6264–6267.
- [45] T. Ghosh, J. Chatterjee, S. Bhakta, *Org. Biomol. Chem.* **2022**, *20*, 7151–7187.
- [46] C. M. Hendrich, K. Sekine, T. Koshikawa, K. Tanaka, A. S. K. Hashmi, *Chem. Rev.* **2021**, *121*, 9113–9163.
- [47] M. Kumar, K. Kaliya, S. K. Maurya, *Org. Biomol. Chem.* **2023**, *21*, 3276–3295.
- [48] J. Labella, G. Durán-Sampedro, M. V. Martínez-Díaz, T. Torres, *Chem. Sci.* **2020**, *11*, 10778–10785.
- [49] T. Matsuda, T. Moriya, T. Goya, M. Murakami, *Chem. Lett.* **2011**, *40*, 40–41.
- [50] Deposition number 2285219 contains the supplementary crystallographic data for this paper. These data are provided free of charge by the joint Cambridge Crystallographic Data Centre and Fachinformationszentrum Karlsruhe Access Structures service.
- [51] R. Bam, W. Yang, G. Longhi, S. Abbate, A. Lucotti, M. Tommasini, R. Franzini, C. Villani, V. J. Catalano, M. M. Olmstead, W. A. Chalifoux, *Org. Lett.* **2019**, *21*, 8652–8656.
- [52] L. Song, G. Tian, L. Van Meervelt, E. V. Van Der Eycken, *Org. Lett.* **2020**, *22*, 6537–6542.
- [53] D. B. Walker, J. Howgego, A. P. Davis, *Synthesis* **2010**, 3686–3692.
- [54] T. Nakae, R. Ohnishi, Y. Kitahata, T. Soukawa, H. Sato, S. Mori, T. Okujima, H. Uno, H. Sakaguchi, *Tetrahedron Lett.* **2012**, *53*, 1617–1619.
- [55] D. Lorbach, M. Wagner, M. Baumgarten, K. Müllen, *Chem. Commun.* **2013**, *49*, 10578–10580.
- [56] A. Suárez, S. Suárez-Pantiga, O. Nieto-Faza, R. Sanz, *Org. Lett.* **2017**, *19*, 5074–5077.
- [57] D. Garayalde, G. Rusconi, C. Nevado, *Helv. Chim. Acta* **2017**, *100*, e1600333.
- [58] P. Barrio, M. Kumar, Z. Lu, J. Han, B. Xu, G. B. Hammond, *Chem. Eur. J.* **2016**, *22*, 16410–16414.
- [59] M. Tasiór, B. Koszarna, D. C. Young, B. Bernard, D. Jacquemin, D. Gryko, D. T. Gryko, *Org. Chem. Front.* **2019**, *6*, 2939–2948.
- [60] B. Dereka, A. Rosspeintner, M. Krzeszewski, D. T. Gryko, E. Vauthey, *Angew. Chem. Int. Ed.* **2016**, *55*, 15624–15628.
- [61] Y. M. Poronik, G. V. Baryshnikov, I. Deperasińska, E. M. Espinoza, J. A. Clark, H. Ågren, D. T. Gryko, V. I. Vullev, *Commun. Chem.* **2020**, *3*, 190.
- [62] M. Krzeszewski, D. T. Gryko, *J. Org. Chem.* **2015**, *80*, 2893–2899.
- [63] C. Adamo, D. Jacquemin, *Chem. Soc. Rev.* **2013**, *42*, 845–856.
- [64] O. Christiansen, H. Koch, P. Jørgensen, *Chem. Phys. Lett.* **1995**, *243*, 409–418.
- [65] C. A. Guido, A. Chrayteh, G. Scalmani, B. Mennucci, D. Jacquemin, *J. Chem. Theory Comput.* **2021**, *17*, 5155–5164.
- [66] M. Krzeszewski, P. Świder, Ł. Dobrzycki, M. K. Cyrański, W. Danikiewicz, D. T. Gryko, *Chem. Commun.* **2016**, *52*, 11539–11542.
- [67] M. Krzeszewski, K. Sahara, Y. M. Poronik, T. Kubo, D. T. Gryko, *Org. Lett.* **2018**, *20*, 1517–1520.
- [68] C. L. Deng, J. P. Bard, J. A. Lohrman, J. E. Barker, L. N. Zakharov, D. W. Johnson, M. M. Haley, *Angew. Chem. Int. Ed.* **2019**, *58*, 3934–3938.
- [69] APEX3 V2019, Bruker Nano, Inc, Program for the Solution of Crystal Structures, Madison, WI, USA **2019**.

- [70] SAINT V8.40 A, Bruker Nano, Inc, Software package for the Solution of Crystal Structures, Madison, WI, USA **2019**.
- [71] SADABS V2016/2, Bruker Nano, Inc, Program for the solution of Crystal Structures **2019**.
- [72] G. M. Sheldrick, *Acta Crystallogr. Sect. A* **2015**, *71*, 3–8.
- [73] G. M. Sheldrick, *Acta Crystallogr. Sect. C* **2015**, *71*, 3–8.
- [74] D. C. Creagh, W. J. McAuley, *International Tables for Crystallography*, Vol C (Ed.: A. J. C. Wilson), Kluwer: Dordrecht **1992**, pp. 200–206.
- [75] C. F. Macrae, I. J. Bruno, J. A. Chisholm, P. R. Edgington, P. McCabe, E. Pidcock, L. Rodriguez-Monge, R. Taylor, J. van de Streek, P. A. Wood, *J. Appl. Crystallogr.* **2008**, *41*, 466–470.
- [76] M. J. Frisch, et al., *Gaussian 16, revision C.01*, Gaussian Inc.: Wallingford, CT **2019**.
- [77] F. Weigend, R. Ahlrichs, *Phys. Chem. Chem. Phys.* **2005**, *7*, 3297–3305.
- [78] S. Grimme, J. Antony, S. Ehrlich, H. Krieg, *J. Chem. Phys.* **2010**, *132*, 154104.
- [79] Y. Zhao, D. G. Truhlar *Theor. Chem. Acc.* **2008**, *120*, 215–241.
- [80] A. V. Marenich, C. J. Cramer, D. G. Truhlar, *J. Phys. Chem. B* **2009**, *113*, 6378–6396.
- [81] CYLview20, C. Y. Legault, *Visualization and analysis software for Computational chemistry*, Université de Sherbrooke **2020** (<http://www.cylview.org>).
- [82] M. J. Frisch, et al., *Gaussian 16, revision A.03*, Gaussian Inc.: Wallingford, CT **2016**.
- [83] J. Tomasi, B. Mennucci, R. Cammi, *Chem. Rev.* **2005**, *105*, 2999–3094.
- [84] A. D. Laurent, D. Jacquemin, *Int. J. Quantum Chem.* **2013**, *113*, 2019–2039.
- [85] TURBOMOLE V7.3/V7.5, a development of University of Karlsruhe and Forschungszentrum Karlsruhe GmbH, **1989–2007**; TURBOMOLE GmbH, can be found under <http://www.turbomole.com>.
- [86] D. Jacquemin, I. Duchemin, X. Blase, *J. Chem. Theory Comput.* **2015**, *11*, 5340–5359.
- [87] J. Cerezo, F. Santoro, FCClasses 3.0, can be found under <http://www.pi.iccom.cnr.it/fcclasses>.
- [88] J. Cerezo, F. Santoro, *J. Comput. Chem.* **2023**, *44*, 626–643.
- [89] F. Santoro, D. Jacquemin, *WIREs Comput. Mol. Sci.* **2016**, *6*, 460–486.

Manuscript received: August 2, 2023

Accepted manuscript online: October 12, 2023

Version of record online: November 2, 2023